論文 / 著書情報
Article / Book Information

題目(和文)	
Title(English)	Synthesis of polyamide-hydroxyapatite nanocomposites and their properties associated with filler shape
著者(和文)	奥村知世
Author(English)	Tomoyo Okumura
出典(和文)	学位:博士(工学), 学位授与機関:東京工業大学, 報告番号:甲第11607号, 授与年月日:2020年9月25日, 学位の種別:課程博士, 審査員:扇澤 敏明,森川 淳子,早川 晃鏡,松本 英俊,淺井 茂雄
Citation(English)	Degree:Doctor (Engineering), Conferring organization: Tokyo Institute of Technology, Report number:甲第11607号, Conferred date:2020/9/25, Degree Type:Course doctor, Examiner:,,,,
学位種別(和文)	博士論文
Category(English)	Doctoral Thesis
種別(和文)	要約
Type(English)	Outline

Doctoral Dissertation

(Abstract)

Synthesis of polyamide-hydroxyapatite nanocomposites and their properties associated with filler shape

Tomoyo OKUMURA

School of Materials and Chemical Technology
Department of Materials Science and Engineering
Tokyo Institute of Technology

July 2020

Table of contents

Chapter 1, General Introduction

Engineering plastics and polyamide 66

Engineering plastic market is one of the growing markets in the industry, whose average growth rate from 2017 to 2022 is expected to be 4.3 % on a monetary basis [1]. Demand for engineering plastic is increasing in recent years. Engineering plastic market mainly consists of general-purpose engineering plastics which are defined by the features as high heat durability (over 100 ^{o}C), high tensile strength (over 50 MPa), and high flexural modulus (over 2.4 GPa); polycarbonate (PC), modified polyphenylene ether (m-PPE), polyamide 6 (PA6), polyamide 66 (PA66), polyoxometalate (POM), polybutylene terephthalate (PBT), and glass fiber-reinforced polyethylene terephthalate (GF-PET). The application is mainly for automobile components, electronics parts, industrial machinery, and medical use.

PA66 is expected to show the biggest growth in the market, whose average growth rate from 2017 to 2022 is expected to be 6.1 % on a monetary basis [1]. PA is defined as the polymer which has repeating amide group. PA66 is the first industrialized polyamide by DuPont and still representative polyamide in today's market. PA66 shows high mechanical properties and heat durability compared to other engineering plastics (Table 1-1) [2]. Especially the glass fiber (GF) reinforced PA66 shows superior mechanical properties and heat durability because the interaction between each PA66 polymer chain is strong due to hydrogen bonds of amide group and PA66 can retain its toughness even with GF reinforcement and maximize the composite properties. However, because of the amide groups, the water absorption rate of PA66 is high. It is important to keep it in mind to select the PA66 application. PA66 is mainly used for automobile components and electronics parts, especially for automobile components in Japan. PA66 is used as a metal (aluminum) substitute in engine compartment for vehicle weight saving; for example, engine head cover, cylinder head cover, intake manifold, and charge air duct. To substitute metal parts, high mechanical properties such as strength, toughness, and rigidity are required. Demand of PA66 is expected to increase and to develop the improved PA66 product is desired.

Table 1-1 Comparison of representative engineering plastics including PA66 [2].

Neat polymer							
		PA6	PA66	PBT	POM	PC	m-PPE
Tm	[°C]	220	**260**	224	180	-	-
Tg	[°C]	50	50	22	-56	150	-
Water absorption (23 °C, 24 h)	[%]	1.8	**1.3**	0.08	0.22	0.24	0.07
Tensile strength	[kg/cm^2]	740	**880**	560	610	630	650
Tensile elongation	[%]	200	60	300	60	100	60
Izod (notch)	[kg-cm/cm]	5.6	4	4	6.5	13	27
HDT (18.6 kg/cm^2)	[°C]	63	70	58	123	135	130
RTI	[°C]	105	105	120	80	110	100
Flame retardancy (UL94)		V-2	**V-2**	HB	HB	V-2	V-0
GF 30 wt% reinforced							
		PA6	PA66	PBT	POM (GF 25 wt%)	PC	m-PPE
Water absorption (23 °C, 24 h)	[%]	1.2	**1.0**	0.07	0.29	0.2	0.06
Tensile strength	[kg/cm^2]	1600	**1700**	1400	1280	1250	1200
Tensile elongation	[%]	5	**5**	4	3	4	5
Izod (notch)	[kg-cm/cm]	11	8	7	8.5	15	12
HDT (18.6 kg/cm^2)	[°C]	190	**240**	210	163	145	140
RTI	[°C]	115	**125**	140	100	130	110
Flame retardancy (UL94)		HB	HB	HB	HB	V-2	HB~V-1

PA nanocomposite

Nanocomposite is defined as the material which contains nanosize dispersed filler in the matrix. “Nanosize” means approximately from 1 nm to 1000 nm, mainly from 1 nm to 200 nm [3]. Nanocomposite could be classified in terms of filler shape as zero dimensional (0D) filler, one dimensional (1D) filler, and two dimensional (2D) filler (Fig. 1-1).

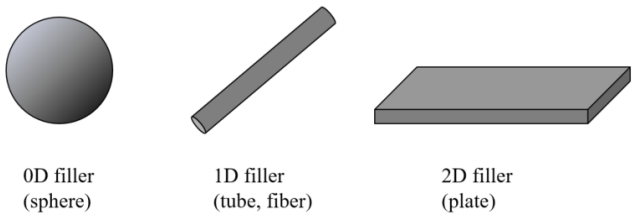

Fig. 1-1 Schematic illustration of nanofiller shape as 0D, 1D, and 2D.

Many kinds of nanofillers have been studied and they increased the composite properties such as mechanical properties, conductivity, barrier properties, flame retardancy, and heat durability. Nanofiller shape is important for the composite property, for example, high L/D filler (1D or 2D filler) was favorable to increase the conductivity because it was easier for high L/D filler to make filler network (percolation). Especially, composite mechanical properties were important indexes for nanofiller effect and each nanofiller (0D, 1D, and 2D) showed different effect. It is the big advantage for 0D filler that the composite does not show anisotropy. It is also the big advantage for 0D filler that it could be mixed with other additive by melt kneading for 0D filler could retain its shape during melt kneading, while 1D or 2D filler might decrease its L/D after melt kneading. 1D filler is the most effective filler to increase mechanical properties, especially to increase the tensile strength by its high L/D. 2D filler could increase mechanical properties, especially increase flexural properties. In terms of composite mechanical properties, it is important to control the filler shape.

In addition, it is also important for improved mechanical properties to increase the interface adhesion between polymer and filler. For that purpose, the surface treatment of nanofiller was conducted before the nanocomposite synthesis. Surface treatment could improve filler dispersion and this also contribute the increase of mechanical properties.

The number of research and publication of polyamide nanocomposite is increasing year by year in recent two decades [4]. Representative example of PA and 0D filler nanocomposite is PA and titanium dioxide nanocomposite [5], PA and barium titanate nanocomposite [6, 7], PA and aluminum oxide nanocomposite [8], PA and zinc oxide nanocomposite [9, 10], PA and silver nanocomposite [11], and PA and POSS nanocomposite [12, 13]. Metal oxide nanoparticle is main filler of PA and 0D filler nanocomposite. Representative example of PA and 1D filler nanocomposite is PA and carbon nanotube (CNT) nanocomposite [14, 15], PA and halloysite nanotube (HNT) nanocomposite [16], and PA and titanium oxide nanotube (TNT) nanocomposite [17, 18]. CNT is mainly studied as the filler of PA and 1D filler nanocomposite. Representative example of PA and 2D filler nanocomposite is PA and clay nanocomposite [19, 20], and PA and graphene nanocomposite [21, 22]. PA and clay nanocomposite is one of the representative polymer nanocomposites, especially PA 6 and clay nanocomposite is widely studied [23].

There are many excellent PA nanocomposites produced by previous studies. However, we think three

important problems are left. First, most nanocomposites can be made only from nanosubstance. Raw materials for nanocomposites explained above are nanosubstance [5-23]. Nanosubstance is harmful for health and it is strictly regulated to use in industrial production process. Special equipment is required to use nanosubstance and it would increase the composite production cost. In addition, nanosubstance itself is usually expensive and increase the composite preparation cost. Second, most current nanofillers have low affinity for PA and surface pre-treatment is required to demonstrate the nanofiller effect sufficiently [5, 14, 15, 19-23]. Surface pre-treatment needs cost and production time. Third, filler shape could not be controlled during production process. For example, we need to fabricate titanium oxide nanotube (1D filler) as raw material for PA-titanium oxide nanotube composite [17, 18]. If we use titanium oxide nanoparticle (0D filler) as raw material, we just obtain PA-titanium oxide nanoparticle composite and the mechanical properties are different from PA-titanium oxide nanotube composite [18]. As discussed above, filler shape is important for composite properties, but the shape of nanosubstance as raw material restricts the composite filler shape. 0D nanosubstance can only be used as raw material for PA and 0D filler nanocomposite. Nanocomposite of PA and 1D or 2D nanofiller could not be obtained from 0D nanosubstance by conventional method (Fig. 1-2). However, it is desirable for industrial production to obtain PA nanocomposite with 0D, 1D, and 2D filler without fabricating the 0D, 1D, and 2D nanofiller as raw material before the production.

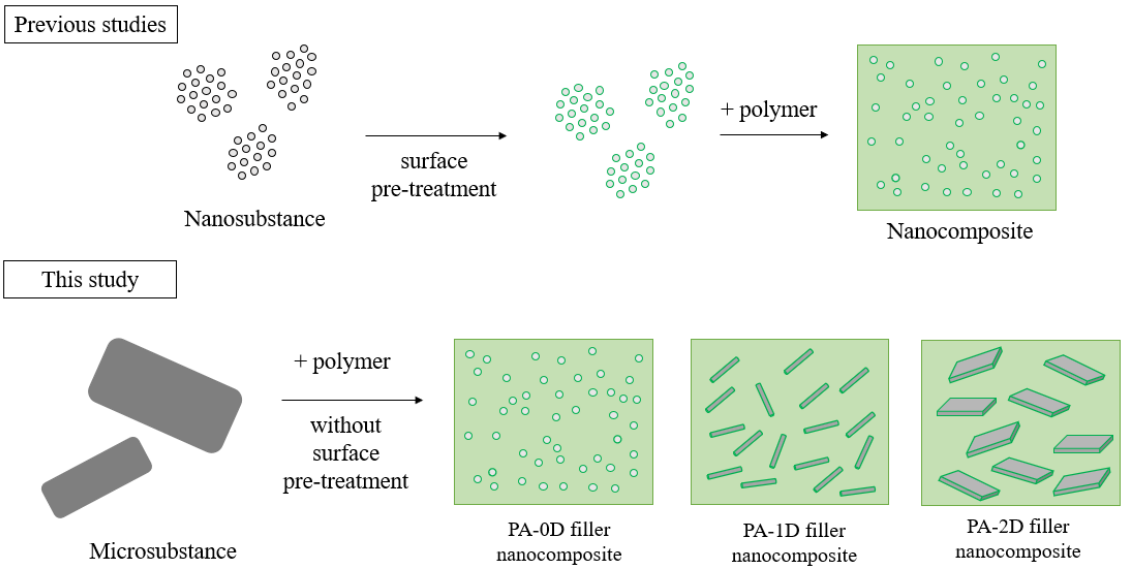

Fig. 1-2 Schematic illustration of previous studies and this study which could synthesize nanocomposite from micro size substance, generate interface without surface pre-treatment, and control the filler shape.

Objective of this thesis

The objective of this thesis is to solve those problems and synthesize novel PA nanocomposite. In

this study, we report the novel nanocomposites and their production process with three advantages against the current PA nanocomposites (Fig. 1-2). First, our PA nanocomposites were made from micro size raw materials. Micro size raw materials became nanosubstance during composite synthesis process without exposure to outside the system. No special equipment to treat nanosubstance was needed. Furthermore, we used generic, low-cost micro size substance as raw materials. Second, the interface bound layer between PA and nanofiller was generated autonomously during the synthesis without surface pre-treatment. This interface enabled the good filler dispersion and high mechanical properties. Third, filler shape was controlled as 0D, 1D, and 2D without complicated operation. In short, we could change the filler shape as 0D, 1D, and 2D by just changing the raw material formulation.

Hydroxyapatite as the nanocomposite filler

Hydroxyapatite (HAp: $Ca_{10}(PO_4)_6(OH)_2$) was selected as the nanocomposite filler for this thesis. As a main inorganic constituent of hard tissues of the human body, HAp has been eagerly studied in the field of biomaterials. Synthesis process of HAp itself was variously studied and had been established. There were many related studies including polymer and HAp composite. HAp-reinforced polyamide was well studied in relation to artificial bones (Fig. 1-3) [24-26]. Mehrabanian et al. adopted an interfacial polymerization method of PA66 to produce nanostructured composites with nano HAp via in situ polymerization [27]. Menon et al. synthesized HAp nanoparticles through a wet chemical reaction and incorporated the HAp into the polymer by melt kneading [28]. Li et al. prepared PA6–HAp composite via in situ hydrolytic ring-opening polymerization of ε-caprolactam in the presence of aqueous HAp slurry [29, 30]. Zhang et al. produced HAp-reinforced PA66 composites by the mixing of PA66 solution and HAp. They also produced carbon-fiber-reinforced PA66-HAp nanocomposite and evaluated the property [31, 32]. Jie et al. prepared PA66-HAp composite using HAp slurry and PA66 solution [33]. Those previous studies were not conducted in the point of solving three PA nanocomposite problems shown above and could not solve them, but they gave us important suggestion to inspire this study.

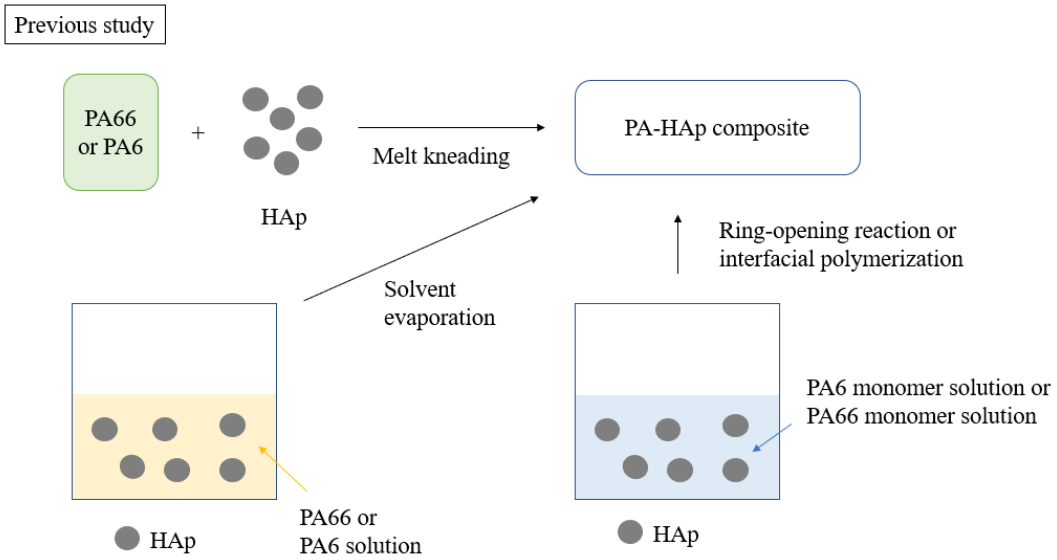

Fig. 1-3 Schematic illustration describing the previous studies of PA-HAp composite.

Human body itself also inspired our study. Bone in the human body is analogue of polymer nanocomposite. Human bone is known as the nanocomposite of hydroxyapatite and collagen (Fig. 1-4) [34]. Collagen molecule ties hydroxyapatite particle and worked as stress transmission bond. When the stress was added to the bone, collagen molecule was strained. This is the reason of bone toughness. Collagen molecule is thought to be interacted with HAp surface through peptide molecule. HAp was expected to interact PA as well as collagen by amide groups. This mechanical property improvement from polymer-filler interaction is desirable for PA nanocomposite.

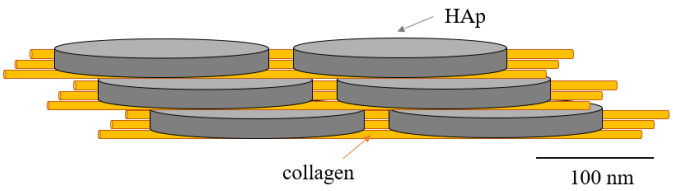

Fig. 1-4 Schematic illustration of human bone which consisted of HAp and collagen.

One-pot synthesis strategy

Initially, PA66-HAp composite was produced by conventional melt kneading of PA66 and HAp reagents which were aggregates of nanometer-sized crystals. The crystals were expected to be dispersed in PA66 by melt kneading, but HAp aggregates remained in the composite (Fig. 1-5). It was the same result of other nanofillers which were difficult to disperse in the matrix polymer by just mixing due to the high cohesive energy of the filler itself. Chemical surface treatment of HAp might work, which was the same solution for many nanofillers. However, it would increase the preparation cost and time.

Fig. 1-5 Schematic illustration of PA-HAp composite with aggregated HAp produced by melt kneading.

Fukushima et al. reported PA6 and montmorillonite nanocomposite prepared through in situ polymerization of PA6 and cation exchanged montmorillonite (Fig. 1-6) [35]. PA6 intercalated montmorillonite compound was obtained through ε-caprolactam intercalation to montmorillonite layer and swelling by polymerization. In situ polymerization with filler is one solution to obtain polyamide nanocomposite with fine filler dispersion.

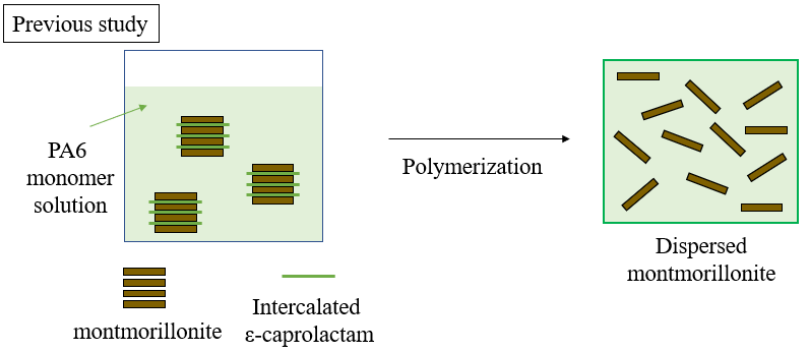

Fig. 1-6 Schematic illustration of PA6-montmorillonite composite with dispersed montmorillonite produced through ε-caprolactam intercalation to montmorillonite layer and swelling by polymerization.

Apart from that, Huang et al. reported the nano-crystal HAp formation on polyamide surface [36]. Calcium ion which was chelated by carboxyl end group of PA matrix played the role as foundation of HAp nano-crystal growth. According to those previous studies, we thought that HAp nano-crystal growth could occur during simultaneous synthesis of PA66 and HAp in one reaction vessel. Fig. 1-7 shows the chemical reaction formula for HAp and PA66, both of which were dehydration reaction by heat.

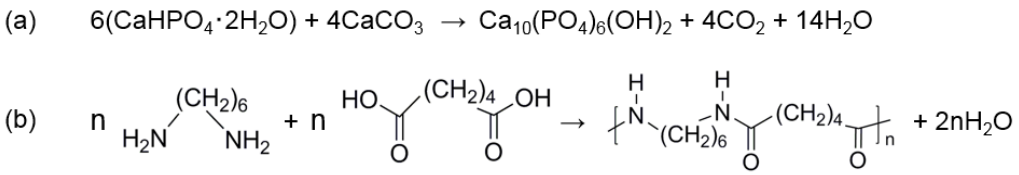

Fig. 1-7 (a) HAp synthesis and (b) PA66 polycondensation, both of which were dehydration reaction by heat.

Simultaneous synthesis of HAp and PA66 in one reaction vessel was carried out and we called this new scheme as "one-pot synthesis." "One-pot synthesis" indicates that the two chemical reactions shown in Fig. 1-7 were performed in one reaction vessel in a mixed state under the conditions shown in Fig. 1-8, which is the standard PA66 polymerization condition. The synthesis was started at room temperature in a reaction vessel, and the temperature was increased. The "condensation phase" was conducted below 150 °C to evaporate the solvent water and concentrate the monomer. Then, the temperature was increased gradually to 280 °C. The condensation phase was conducted at 0.2 MPa. The pressure was then increased and maintained at 1.8 MPa to allow polymerization ("polymerization phase"). As the reaction proceeded, the pressure was decreased to below 0.2 MPa by releasing water vapor ("Depressure phase").

$CaHPO_4 \cdot 2H_2O$ (dicalcium phosphate dihydrate: DCPD) and $CaCO_3$ were selected as HAp raw materials, and hexamethylene diamine and adipic acid were used as monomers for PA66.

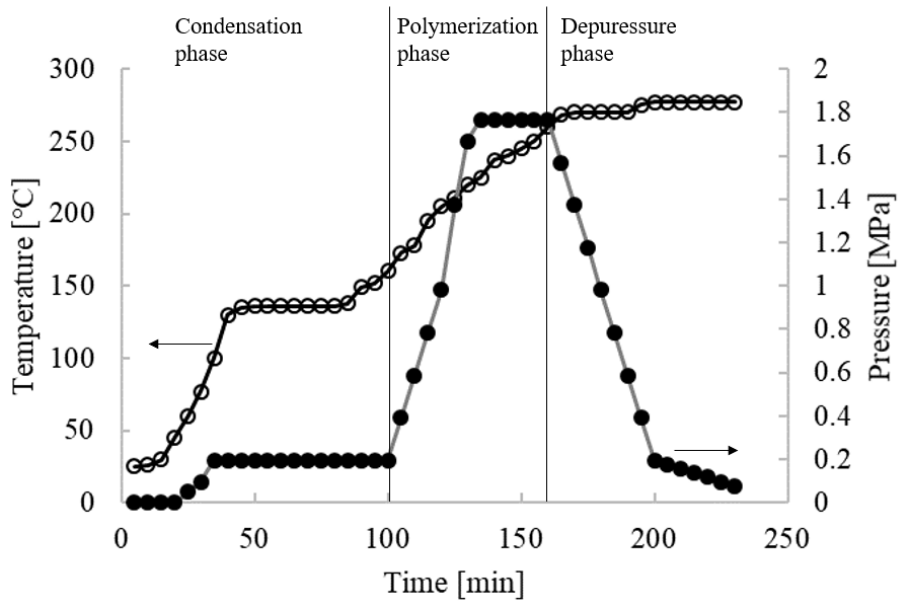

Fig. 1-8 Synthesis condition for PA66 which was assumed as the one-pot synthesis reaction condition.

There was no previous study which investigated HAp synthesis at PA66 polymerization condition with high temperature and high pressure shown in Fig. 1-8. In addition, coexisting monomer effect must be studied before the one-pot synthesis.

In chapter 2, HAp synthesis reaction under various temperature, time, and coexisting organic molecular and ions were examined at first. Then, new synthesis method was developed to obtain the PA66-HAp nanocomposite. The simultaneous syntheses of PA66 and HAp was performed by extracting H_2O and CO_2 from PA66 monomers and HAp raw materials in one vessel. The surface of DCPD as HAp raw material became porous during the early stage of one-pot synthesis by dissolving and then nanosized HAp precursor was precipitated. The reaction intermediate from DCPD and resultant HAp interacted with PA66 monomer, oligomer, and prepolymer to form PA66-HAp interface polymer (bound polymer). HAp aggregation was prevented by this bound polymer. TEM observation of the formed PA66-HAp composite showed nano HAp particle dispersion. The PA66-HAp nanocomposite showed improved mechanical properties compared with neat PA66 because of the fine HAp dispersion and strong interface adhesion between PA66 and HAp. PA and 0D (spherical shape) HAp nanocomposite was synthesized in the chapter.

In chapter 3, carbon fiber (CF) reinforced PA-0D HAp nanocomposite (PA-HAp/CF) was produced by melt kneading of CF and PA-0D HAp nanocomposite. PA-HAp/CF composite showed increased strength, toughness, and long-term reliability than CF reinforced PA (PA/CF) composite. To clarify the reason, the fracture behavior of the composite was analyzed by acoustic emission (AE). Glass fiber (GF) reinforced PA-0D HAp nanocomposite (PA-HAp/GF) and GF reinforced PA (PA/GF) composite were also produced and analyzed as references. By comparing the AE results of those composites, synergy effect of CF and HAp was clarified. Nano HAp effect for PA-HAp/CF composite strength, toughness, and long-term reliability was attributed to the interfacial polymer of PA-HAp, that undertook the part of the stress to the composite.

In chapter 4, HAp shape in PA-HAp nanocomposite was controlled to be needle shape to improve mechanical properties. To obtain the needle shape HAp, additional ion effect for the HAp shape formation was studied. HAp shape was changed by adding specific ion to HAp raw material, which accelerate the anisotropic HAp crystal growth. Under specific ion composition, PA66-needle shape HAp composite was obtained by one-pot synthesis. PA and 1D (needle shape) HAp nanocomposite was synthesized in the chapter. The composite showed increased mechanical properties, especially high tensile strength because of the high L/D filler.

In chapter 5, HAp shape in PA-HAp nanocomposite was controlled to be plate shape to improve mechanical properties. Octa-calcium phosphate (OCP) was focused as the intermediate because OCP had plate shape and was expected to convert to plate shape HAp heterogeneously. Also, adipic acid (ADA) intercalated OCP was used as HAp precursor and resultant PA-HAp nanocomposite showed better PA affinity for HAp because intercalated ADA accelerated the bound polymer formation. PA

and 2D (plate shape) HAp nanocomposite was synthesized in the chapter. The PA-plate shape HAp nanocomposite showed increased flexural strength and reduced water absorption rate.

In chapter 6, the discussion is closed with conclusions of this study.

PA nanocomposite is one of the promising materials for industry. The goal of this study is to improve the PA66 properties, especially mechanical properties by nanofiller reinforcement. This study is distinguished from previous studies in terms of; First, autonomous synthesis of nanocomposite from micro size raw material. Second, strong interface creation between matrix and filler without surface pre-treatment. Third, controllable filler shape such as 0D (particle), 1D (needle), and 2D (plate). In this study, nanocomposite of PA66 and HAp was produced by novel synthesis process.

References

[1] Mizoguchi, M., Eds; *Prospect of engineering plastic market and global strategy 2019*, Fuji-keizai, Tokyo, **2019**.

[2] Fukumoto, O., Eds; *Polyamide Handbook*, Tokyo, **1988**.

[3] Okamoto, M., *Current status of technology development and future prospect*, in: Okamoto, M.; Eds; *Polymeric Nanocomposites*, CMC books, Tokyo, **2010**, pp. 1–25.

[4] Francisco, D. L.; Paiva, L. B.; Aldeia, W. *Polymer Composites* **2019**, *40* (3), 851-870.

[5] Bet-Moushoul, E.; Mansourpanah, Y.; Farhadi, Kh.; Tabatabaei, M. *Chem. Eng. J.* **2016**, *283*, 29-46.

[6] Capsal, J. F.; Pousserot, C.; Dantras, E.; Dandurand, J.; Lacabanne, C. *Polymer.* **2010**, *51,* 5207-5211.

[7] Akbar, A.; Riaz, S.; Hussain, S. S.; Naseem, S. *Mater. Today Proc.* **2015**, *2*, 5395-5399.

[8] Ogunniran, E. S.; Sadiku, R.; Ray, S. S.; Luruli, N. *Macromol. Mater. Eng.* **2012**, *297*, 627-638.

[9] Li, X. H.; Kretzschmar, B.; Janke, A.; Häussler, L.; Schneider, K.; Stamm, M. *Adv. Mater. Res.* **2012**, *557-559,* 272-276.

[10] Pal, A.; Dey, T. K.; Singhal, A.; Bindal, R. C.; Tewari, P. K. *RSC adv.* **2015**, *5,* 34134-34151.

[11] Liu, S.; Fang, F.; Wu, J.; Zhang, K. *Desalination* **2015**, *375*, 121-128.

[12] Ayandele, E.; Sarkar, B.; Alexandridis, P. *Nanomaterials* **2012**, *2,* 445-475.

[13] Andrade, R. J.; Huang, R.; Herbert, M. M.; Chiaretti, D.; Ishida, H.; Schiraldi, D. A.; Maia, J. M. *Polymer,* **2014**, *55*, 860-870.

[14] Faghihi, M.; Shojaei, A.; Bagheri, R. *Compos. B,* **2015**, *78*, 50-64.

[15] Ryu, J.; Han, M. *Compos. Sci. Technol.*, **2014**, *102*, 169-175.

[16] Liu, M.; Guo, B.; Du, M.; Chen, F.; Jia, D. *Polymer,* **2009**, *50*, 3022-3030.

[17] Kasuga, T.; Hiramatsu, M.; Hoson, A.; Sekino, T.; Niihara, K. *Langmuir,* **1998**, *14*, 3160-3163.

[18] Kralova, D.; Slouf, M.; Klementova, M.; Kuzel, R.; Kelnar, I. *Mater. Chem. Phys.,* **2010**, *124*, 652-657.

[19] Messersmith, P. B.; Giannelis, E. P. *Chem. Mater.,* **1993**, *5*, 1064-1066.

[20] Vaia, R. A.; Ishii, H.; Giannelis, E. P. *Chem. Mater.,* **1993**, *5*, 1694-1696.

[21] Li, R.; Shi, K.; Ye, L.; Li, G. *Ind. Eng. Chen. Res.*, **2017**, *56*, 13715-13724.

[22] O'Neill, A.; Bakirtzis, C.; Dixon, D. *Eur., Polym. J.*, **2014**, *59*, 353-362.

[23] Usuki, A.; Kojima, Y.; Kawasumi, M.; Okada, A.; Fukushima, Y. Kurauchi, T.; Kamigaito, O. *J. of Material Reserch,* **1993**, *8* (5), 1179-1184.

[24] Bonfeild, W; Behri, J. C.; Doyle, C.; Bowman, J.; Abram, J. *Biomater. Biomech,* **1983***,* 421-426.

[25] Antonis, G. M.; Lyman, M. D.; Freed, L. E.; Langer, R. *Biomaterials,* **1994***, 15*, 55-58.

[26] Liu, Q.; Wijn, J. R.; Groot, K.; Blitterswijk, C. A. *Biomaterials,* **1998**, *19*, 1067-1072.

[27] Mehrabanian, M.; Nasr-Esfahani, M.; Jafari, M. *International Journal of Polymeric Materials,*

2012, *61* (5-8)*,* 558-570.

[28] Menon, D.; Anand, K. A.; Anitha, V. C.; Nair, S. *International Journal of Polymeric Materials,* **2010**, *59* (7-9), 498-509.

[29] Li, L.; Yang, G. *Polymer International,* **2008**, *57* (11), 1226-1234.

[30] Li, L.; Yang, *Polymer International,* **2009**, *58* (4), 380-387.

[31] Zhang, X.; Li, Y.; Lv, G.; Zuo, Y.; Mu, Y. *Polymer Degradation and Stability,* **2006**, *91* (5), 1202-1207.

[32] Zhang, X.; Zhang, Y.; Zhang, X.; Wang, Y.; Wang, J.; Li, M.; Li, H. *Journal of the Mechanical Behavior of Biomedical Materials,* **2015***, 42*, 267-273.

[33] Jie, W.; Yubao, L.; Weiqun, C.; Yi, Z. *Journal of Materials Science,* **2003***,38*(15), 3303-3306.

[34] Fratzl, P.; Gupta, H. S.; Paschalis, E. P.; Roschger, P. *J. Mater. Chem.*, **2004**, *14*, 2115-2123.

[35] Fukushima, Y.; Inagaki, S. *J. of Inclusion Phenomena,* **1987**, *5,* 473-482.

[36] Huang, D.; Yin, M.; Lin, Q.; Qin, Y.; Wei, Y.; Hu, Y.; Lian, X.; Guo, M.; Du, J.; Chen, W. *RSC Advances*, **2017**, *7* (68), 43040-43046.

Chapter 2,
Nanocomposite of polyamide and 0D (spherical shape) hydroxyapatite

Introduction

Reaction process of HAp synthesis from DCPD was well studied for a long time and there were two main proposed mechanisms (Fig. 2-1). First proposed mechanism was the direct transition from DCPD to HAp at solid state. Aoki et al. reported the HAp synthesis from DCPD and monetite [1]. They reported the HAp formation not only under hydrothermal synthesis but also under hot steam (over 300 ^{o}C) reaction. They said that according to the gas phase and solid phase reaction result, the direct transition from DCPD to HAp without DCPD dissolution might occur. Sakashita et al. analyzed the reaction process from DCPD to HAp by XRD [2]. They reported that as the reaction proceed, relative intensity of DCPD (111) peak decreased and relative intensity of HAp (111) increased. In addition, lattice spacing of DCPD (111) (d = 0.305 nm) and HAp (111) (d = 0.388 nm) were close. According to the results, they said that the transition from DCPD to HAp might occur through DCPD (111) phase.

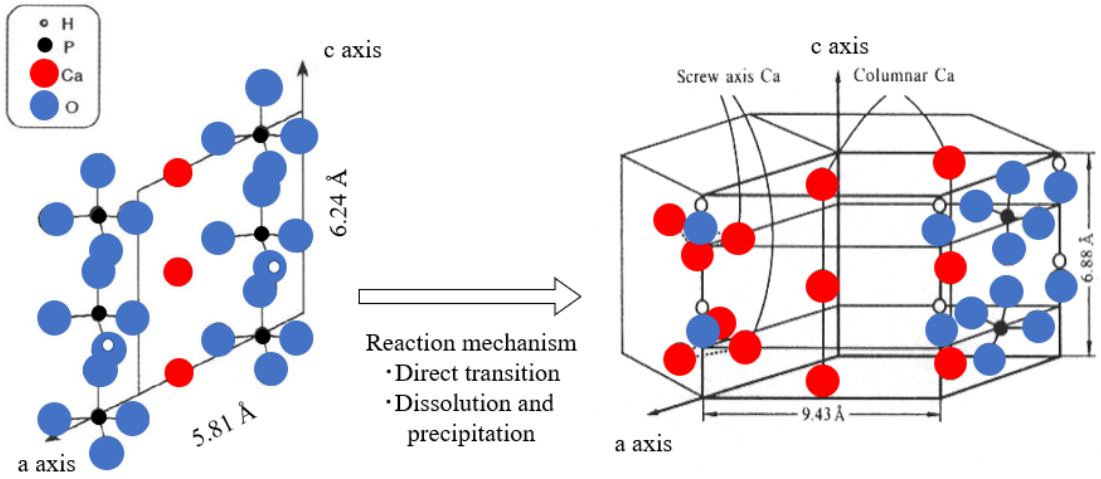

Fig. 2-1 Schematic illustration of proposed mechanisms about reaction process of HAp synthesis from DCPD.

Second proposed mechanism was dissolution and precipitation mechanism. Rocha et al. reported that DCPD surface became porous before it transforms to HAp under basic (alkaline) aqueous media [3]. They reported that nano HAp crystal was generated on the surface of the DCPD. They said that the conversion from DCPD to HAp occurred by surface dissolution of DCPD followed by nucleation and growth of HAp nanocrystal. Onuma reported the AFM analysis of the HAp growth from DCPD [4].

He followed the phase transition process from DCPD to HAp by AFM and concluded that the transition was dissolution and precipitation mechanism because there was no reaction intermediate through the process. He could detect just the dissolution on DCPD and precipitated HAp after the DCPD dissolution. In addition, he calculated the step kinetics coefficient β from AFM analysis, which could be approximated the crystal growth or dissolve speed. The calculated values were; DCPD dissolution $\beta = 0.35\text{-}4.6\times10^{-2}$ cm/s and HAp crystal growth $\beta = 0.4\times10^{-4}$ cm/s. HAp crystal growth speed was less than one hundredth than DCPD dissolving speed. According to the results, he said the direct transition from DCPD to HAp was not likely to occur. To conclude the transition mechanism to HAp from DCPD is not the objective of our study. However, according to previous studies, dissolution and precipitation mechanism is likely to occur even though this might not be the all transition route. It is very important to control the transition mechanism to HAp from DCPD to fabricate the nano HAp and PA-HAp nanocomposite.

There were also some previous studies about how accelerate or decelerate the reaction speed of HAp synthesis from DCPD (Fig. 2-2). Monma reported that reaction process of HAp from DCPD was consisted from two steps [5]. First, structural change from DCPD to nonstoichiometric HAp ($Ca_{10-x}(PHO_4)_x(PO_4)_{6-x}(OH)_{2-x}\cdot nH_2O$ (Ca/P < 1.67)). Then conversion from nonstoichiometric HAp to stoichiometric HAp ($Ca_{10}(PO_4)_6(OH)_2$ (Ca/P = 1.67)) was proceeded. To complete the second process, increasing the Ca/P ratio, adding Ca^{2+} or removing HPO_4^- by increasing pH was very effective. However, he reported that adding Ca^{2+} or increasing pH suppress the proceeding of the first reaction. To complete the HAp generation reaction from DCPD, ionic density and pH was important.

It was reported that organic molecules could mediate the HAp synthesis from DCPD through different mechanisms depending on the nature of interactions between the additive organic molecules and the DCPD phase. Albumin was reported to have retardant effect on DCPD transformation. At first, albumin was bound to calcium ions of DCPD. Then electrostatic interactions between albumin and DCPD surface restricted the dissolution and subsequent precipitation process [6]. In contrast, transformation of DCPD to HAp was promoted in the presence of citrate acid and acidic amino acids by reducing the interfacial energy barrier [7, 8]. Ucar et al. reported that conversion to HAp was suppressed by alginate additives [9]. They also reported that HAp addition to the reaction system as HAp nuclear invalidate the reaction retardant effect of alginate additives. They conclude that alginate additives inhibited the HAp nucleation and did not inhibit the HAp crystal growth. Kumar et al. reported that potassium treatment of DCPD before the reaction accelerated the HAp conversion [10]. DCPD treatment in the KCl bath (r.t., 8 h) resulted the partial substitution of Ca^{2+} to K^+. They said that lattice strain and higher energy state was possible reason of conversion acceleration.

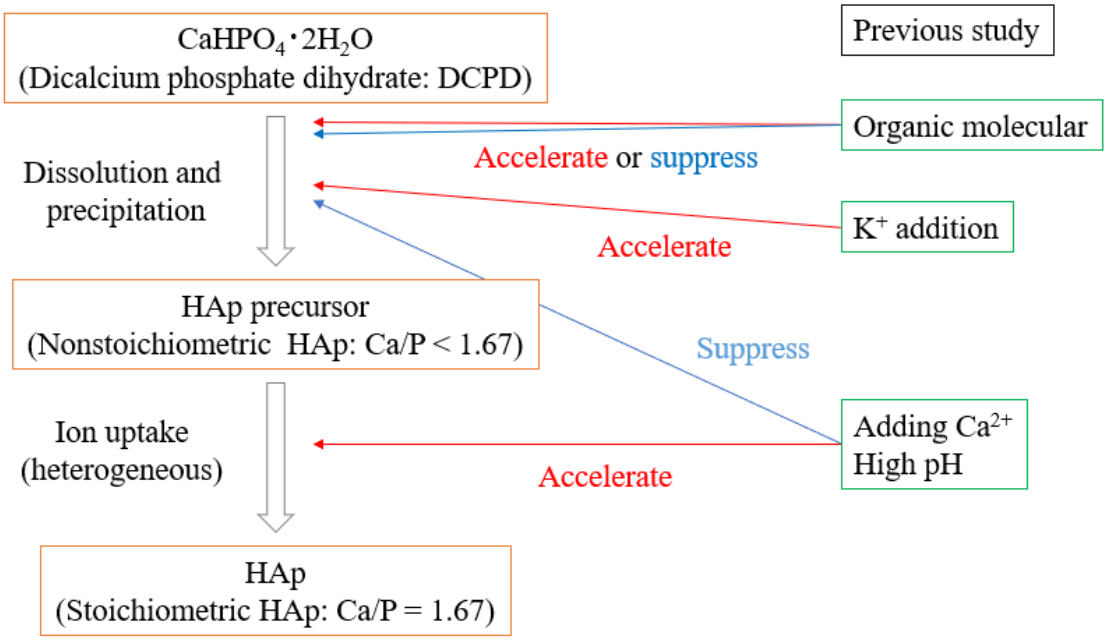

Fig. 2-2 HAp synthesis route from DCPD and factors which accelerated or suppressed the process found by previous studies.

One-pot synthesis was designed as simultaneous reaction of HAp synthesis from DCPD and PA66 polymerization from hexamethylene diamine and adipic acid under the polymerization condition. According to those previous studies, conversion reaction to HAp from DCPD was complicated and easily influenced by the coexisting organic molecular and ions. To confirm the HAp synthesis under the one-pot synthesis reaction condition, HAp synthesis reaction under various temperature, time and coexisting organic molecular and ions were examined. Then, one-pot synthesis was carried out and the synthesis process, morphology and property of resultant product were examined.

Summary of hydroxyapatite synthesis under various conditions

HAp synthesis reaction under various temperature, time, and coexisting organic molecular and ions were examined. According to the results of temperature dependence of HAp synthesis, HAp synthesis was expected to occur mainly at condensation phase. The result of synthesis trial at one-pot synthesis condition without PA monomer showed HAp synthesis as expected. In addition, the effect of coexisting polyamide monomers was investigated in terms of pH and chelating effect. It was possible to synthesize HAp from DCPD with coexisting PA66 monomers. However, adipic acid might suppress the HAp synthesis by inhibiting the Ca^{2+} adsorption to HAp precursor. In addition, the raw material dependence in terms of size, shape, and purity of $CaHPO_4 \cdot 2H_2O$ or $CaCO_3$ was examined. Impurities might affect the HAp crystal growth, but it was possible to synthesize HAp from DCPD and $CaCO_3$ with different size, shape, and purity. HAp synthesis promotion effect of K^+ shown in previous study

was also investigated. However, it was not clear that whether K_2HPO_4 promoted the HAp synthesis or not. In summary, HAp synthesis reaction from DCPD showed good resilience at various conditions and this result supported that HAp was a good filler candidate for one-pot synthesis. Then, we conducted one-pot synthesis from PA66 monomer, DCPD, and $CaCO_3$.

Conclusions

One-pot synthesis of HAp and PA66 was performed to produce PA66-HAp nanocomposite. A precedent HAp synthesis followed by PA66 polymerization during one-pot synthesis was confirmed by XRD and SEM analysis. The nanosized HAp precursor was synthesized during the early stage of PA66 synthesis reaction and then PA66 polymerization proceeded. The HAp raw material was micro meter size, much larger than resultant nanosized HAp. One-pot reaction could produce nanocomposite autonomously from micro meter raw materials, which was the big advantage especially for industrial mass production. FT-IR and TGA analysis showed that the bound polymer between HAp and PA66 was generated during one-pot synthesis. The amount of bound polymer was greater than that achieved by melt kneading and that rich bound polymer enabled the HAp fine dispersion in the PA66-HAp composite. Basic one-pot synthesis condition investigated in this chapter could produce PA-0D (spherical shape) HAp nanocomposite. The shape control of HAp to 1D (needle shape) and 2D (plate shape) was studied in chapter 4 and chapter 5.

PA66-0D HAp nanocomposite produced by one-pot synthesis showed unique properties. The improved mechanical properties of the PA66-0D HAp nanocomposite were attributed to HAp fine dispersion and bound polymer. Not only mechanical properties, but also the heat aging resistance and hot water resistance were increased by HAp reinforcement. HAp stiffness and bound polymer which shared the stress improved the compression creep property. Nanosize, spherical shape HAp decreased the maximum mold shrinkage rate and showed very small anisotropy. Extensional viscosity was increased especially at low share rate, which was the same phenomenon as other nanocomposite like PA6-clay nanocomposite. Friction and wear characteristics were surprisingly increased by increasing the composite modulus because of the HAp itself and higher crystallinity. PA66-HAp nanocomposite is expected to be useful material for industry by taking advantages of those properties.

For the usage of automobile components, which is the biggest market for PA66, mechanical properties and long-term reliability are especially important. We focused on the HAp effect for mechanical properties and long-term reliability at next chapter.

References

[1] Aoki, H.; Kato, K.; Shiba, M. *Shika Rikougaku Zassi*, **1972**, *13* (27), 170-176.

[2] Tanaka, S.; Machinaga, O. *Reserch report A of College of Industrial Technology. Nihon Univ*., **2005**, *38* (2), 35-39.

[3] Rocha, D. N.; Silva, M. H. P; Campos, J. B.; Marcal, R. L. S. B.; Mijares, D. Q.; Coelho, P. G.; Cruz, L. R. *J. of Materials research and Technology,* **2018**, *7* (4)*,* 479-486.

[4] Onuma, K. *J. of the Surface Finishing Society of Japan,* **2000**, *51* (1), 34-41.

[5] Monma, H.; Kaiya, Y. *J. of Materials Science*, **1987**, *22*, 4247.

[6] Xie, J.; Riley, C.; Chittur, K. *J. Biomed. Mater. Res.,* **2001,** *57*, 357-365.

[7] Jiang, W.; Chu, X.; Wang, B.; Pan, H.; Xu, X.; Tang, R. *J. Phys. Chem. B,* **2009**, *113*, 10838-10844.

[8] Chu, X.; Jiang, W.; Zhang, Z.; Yan, T.; Pan, H.; Xu, X.; Tang, R. *J. Phys. Chem. B,* **2011**, *115*, 1151-1157.

[9] Ucar, S.; Bjornoy, S. H.; Bassett, D. C.; Strand, B. L.; Sikorski, P.; Andreassen, J. P. *J. of Crystal Growth*, **2017**, *468,* 774-780.

[10] Kumar, M.; Xie, J.; Chittur, K.; Riley, C. *Biomaterials,* **1999**, *20,* 1389-1399.

Chapter 3,
Mechanical properties and fracture behavior of fiber filler reinforced nanocomposite

Introduction

Mechanical property is one of the most important properties for engineering plastic, especially for those materials which substitute metal parts. Not only the initial value but also the value after some period of usage, so-called long-term reliability is important for practical use. The creep resistance and vibration fatigue resistance were widely tested as the indexes for long-term reliability of PA composite. We confirmed that the compression creep resistance of PA66-spherical shape HAp nanocomposite was increased more than neat PA66. Previously, nanocomposite was reported to improve creep resistance [1-3]. However, only the creep resistance of nanocomposite itself (matrix and nanofiller) was evaluated and the synergetic effect of nanocomposite and inorganic fiber filler for creep resistance improvement did not attract an attention. Inorganic fiber fillers are usually reinforced to PA composite especially for metal substitution usage to increase mechanical properties and thermal characteristics (e.g. HDT). To develop the inorganic fiber filler reinforced PA composite with good long-term reliability is desired. Previous study was conducted to clarify the PA-inorganic fiber filler composite fatigue mechanism and showed that when PA/GF composite vibration fatigue resistance test was conducted, fracture process started at the PA and GF interface (Fig. 3-1) [4]. Furthermore, the crack proceeded through the composite. At last, the crack connected with each other and the material was broken. The modulus difference between polymer and filler was large and when the composite was stressed, the stress distribution tended to show the highest value at the polymer-filler interface, and the interface was likely to deform at the early stage of the fracture. To improve the long-term reliability, many studies were conducted and one of the main methods was to improve the adhesion between PA and filler interface. By the GF surface treatment of silane coupling agent and sizing agent, the vibration fatigue resistance of PA/GF composite was improved [5]. In these days, the metal substitution by polymer to save the vehicle weight became more important for low fuel consumption. Studies for improving long-term reliability of PA composite draw much attention for the application to vehicle parts. To develop the material with high long-term reliability, it is important to understand the fracture behavior of the material.

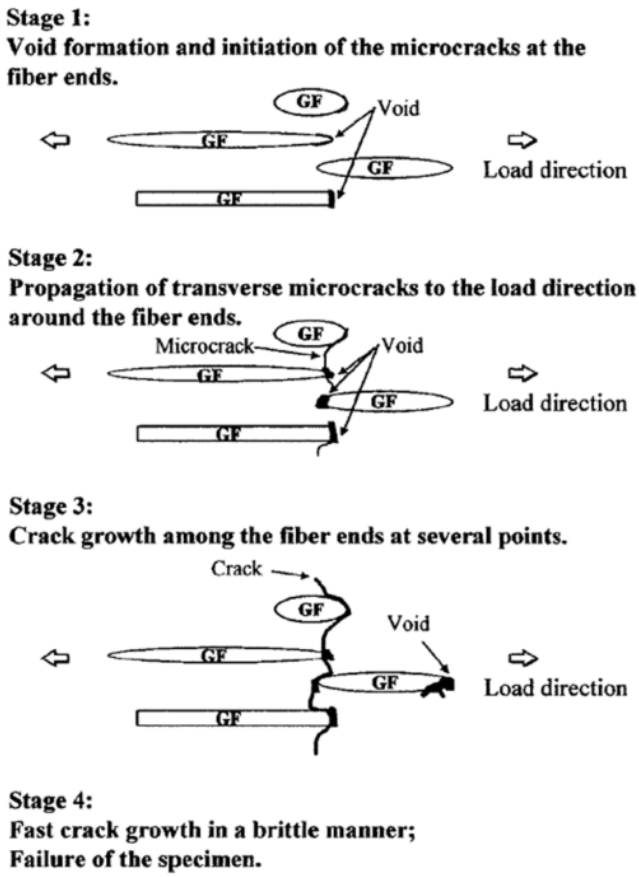

Fig. 3-1 Proposed process of PA/GF fatigue test which shows three stages of fracture (a) void formation, (b) microcrack propagation, (c) crack growth (Noda, K. et al., 2001) [4].

The fracture behavior of polymer was well studied for a long time. It is said that polymer fracture was at first started as craze formation [6]. Then the “stable crack propagation” was proceeded. At last, “unstable crack” propagated and polymer fracture was occurred before the fracture (Fig. 3-2).

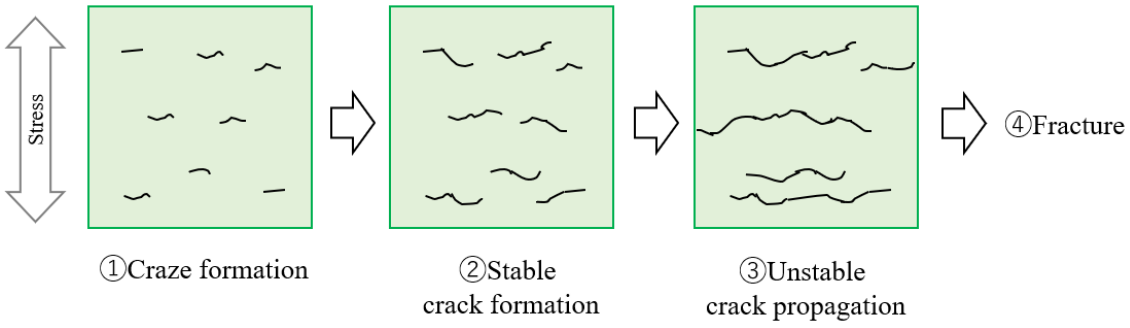

Fig. 3-2 Schematic illustration describing fracture behavior of polymer.

The crack propagation process of PA 66 was studied and it was found that craze or crack went through inside the spherulite. At high crystalline PA, craze was preferably formed at the initial stage of fracture [7]. On the other hand, at low crystalline PA, crack was mainly formed even at the initial stage of fracture. High crystalline PA was more durable for fatigue vibration test than low crystalline PA and it was said in previous study that craze formation was important factor. The additive effect for craze propagation was also studied and it was found that rubber particle could stop craze propagation (Fig. 3-3) [8].

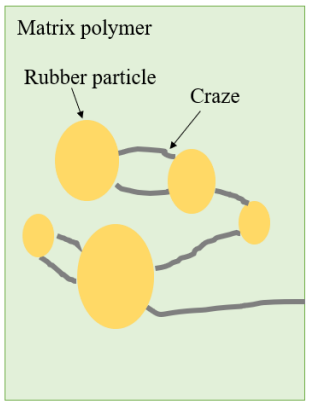

Fig. 3-3 Schematic illustration of rubber particle effect for stopping craze propagation [8].

Not only the rubber but also the nanoparticle could change the craze formation and propagation. The previous study showed that the nanoclay addition could change the fracture behavior of carbon/glass/epoxy hybrid composite [9]. The study discussed only the microscopic fracture behavior change but it was expected that fracture behavior change was the result of craze formation or propagation change by added nanoclay. PA-HAp nanocomposite discussed in chapter 2 was the novel nanocomposite synthesized by novel one-pot synthesis method and it was expected that this nano HAp in PA matrix could also change the fracture behavior of the composite. In previous study, nanofiller effect for polymer fracture behavior was studied. Nanoparticle was added to PMMA to increase mechanical property [10, 11]. The nanoparticle changed the fracture behavior of the PMMA composite (Fig. 3-4). The fracture behavior of composites was studied by acoustic emission (AE).

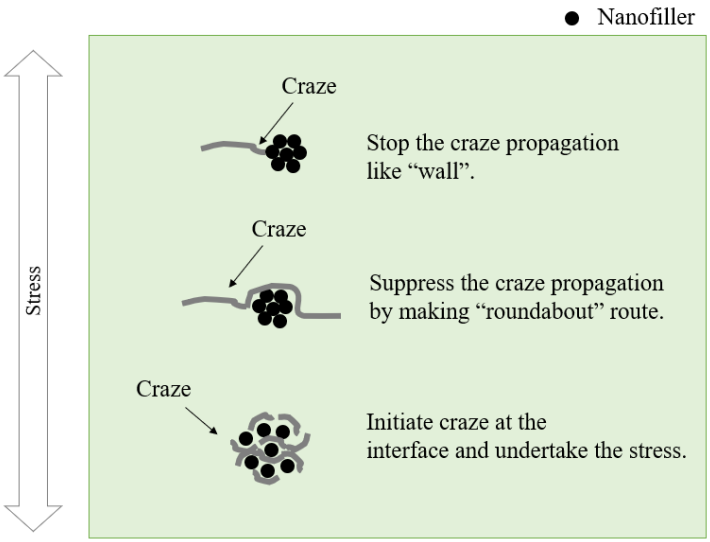

Fig. 3-4 Schematic illustration of nanofiller effect according to previous studies, which suppress the material fracture [10, 11].

AE is one of the useful indexes to study the matrix fracture behavior and used for polymer composite study. Elastic wave released by material fracture was detected by AE sensor (Fig. 3-5). Wave number and wave energy calculated by amplitude and duration time were used for analysis as index of fracture behavior (Fig. 3-6).

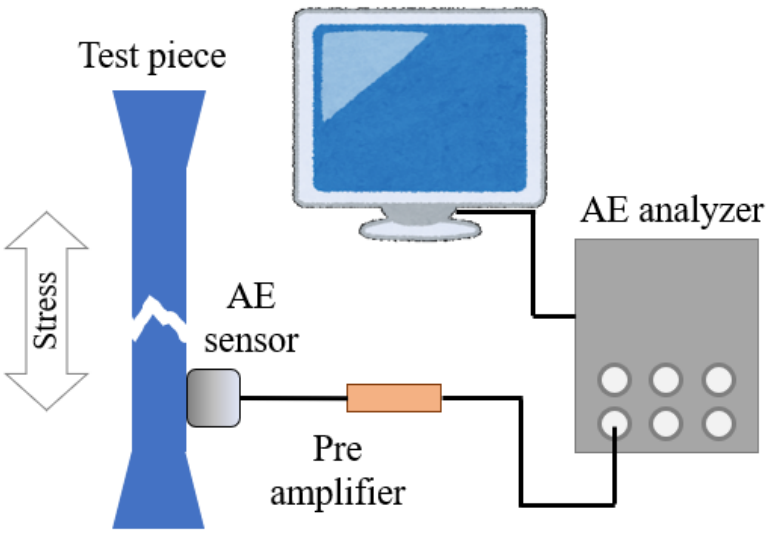

Fig. 3-5 Schematic illustration of AE analysis system.

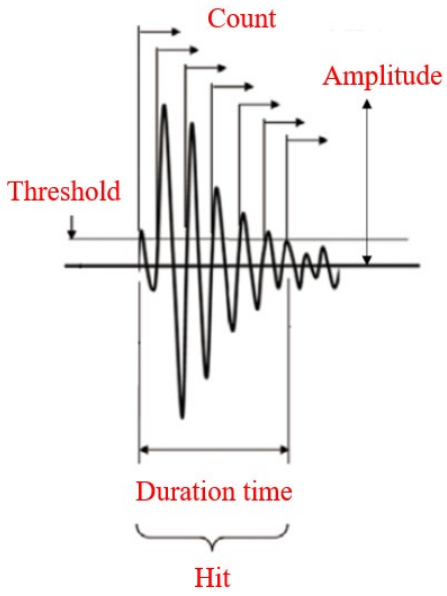

Fig. 3-6 Schematic illustration of AE results.

Jinen et al. studied AE of PA/CF composite intensively [12-15]. They revealed that fracture behavior of polymer which was described as three stages of craze formation, stable crack formation, and unstable clack propagation could be detected by AE. Semi-logarithmic plot of AE total events showed two inflection points that showed fracture process had three stages, which corresponded to the craze formation stage, stable crack formation stage, and unstable crack propagation stage (Fig. 3-7). After unstable crack propagation stage, test piece was broken. Apart from them, Karger-Kocsis et al. studied the fracture behavior of PA/GF composite (glass fiber mat reinforced PA) by AE [16].

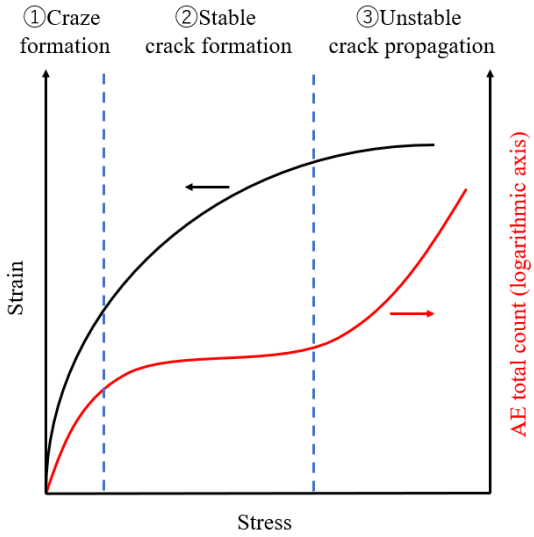

Fig. 3-7 Schematic illustration of fracture behavior of polymer which was described as three stages detected by AE.

In addition, AE emission could be divided into three types by AE duration time and AE amplitude, such as AE by matrix fracture, AE by PA and filler interface fracture, and AE by filler fracture (Fig. 3-8) [17]. Those previous studies indicated that AE is the effective tool to study the fracture behavior of PA composite.

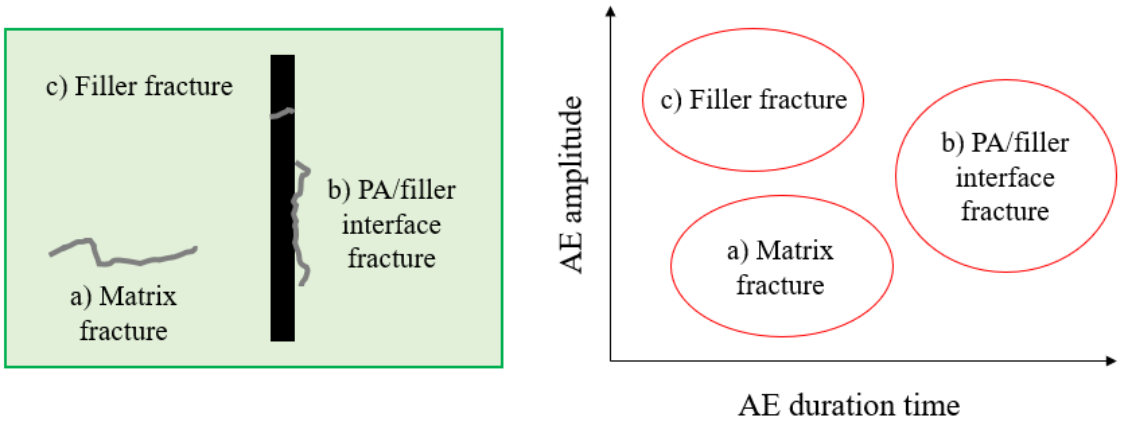

Fig. 3-8 Schematic illustration describing that AE emission could be divided into three types by AE duration time and AE amplitude.

In this study, the mechanical properties and the long-term reliability of inorganic fiber filler reinforced PA-0D HAp nanocomposite was evaluated and it was found that nano HAp improved strength, toughness, and creep resistance of PA/CF composite. To clarify the reason, fracture behavior of PA-HAp/CF composite was studied by AE.

Summary of AE analysis

Fig. 3-9 and Fig. 3-10 are schematic illustrations of fracture behavior of the composites. The difference of fracture behavior of each composite could be explained by modulus difference and interface adhesiveness.

For PA/CF composite, the fracture was started at the interface of filler polar direction and matrix of near filler polar direction (initial craze formation stage). Then, the crack was propagated along PA/CF interface at stable crack formation stage. At last, unstable crack propagation occurred by connecting PA/CF interface fracture before the fracture. For PA-HAp/CF composite, fracture was also started at filler polar direction interface and matrix of near filler polar direction (initial craze formation stage). Then, the crack was propagated along PA/CF interface (stable crack propagation stage). Because the modulus difference of PA and HAp was much smaller than that of PA and CF, and the interface adhesiveness was poor, PA/CF interface fracture was occurred preferentially than PA/HAp interface fracture. Only small part of PA/HAp interface was peeled during this stage and HAp did not act as crack connection point. At last, unstable crack propagation occurred by connecting PA/CF interface fracture before the composite fracture. HAp might stop the craze propagation like walls and delayed the final fracture.

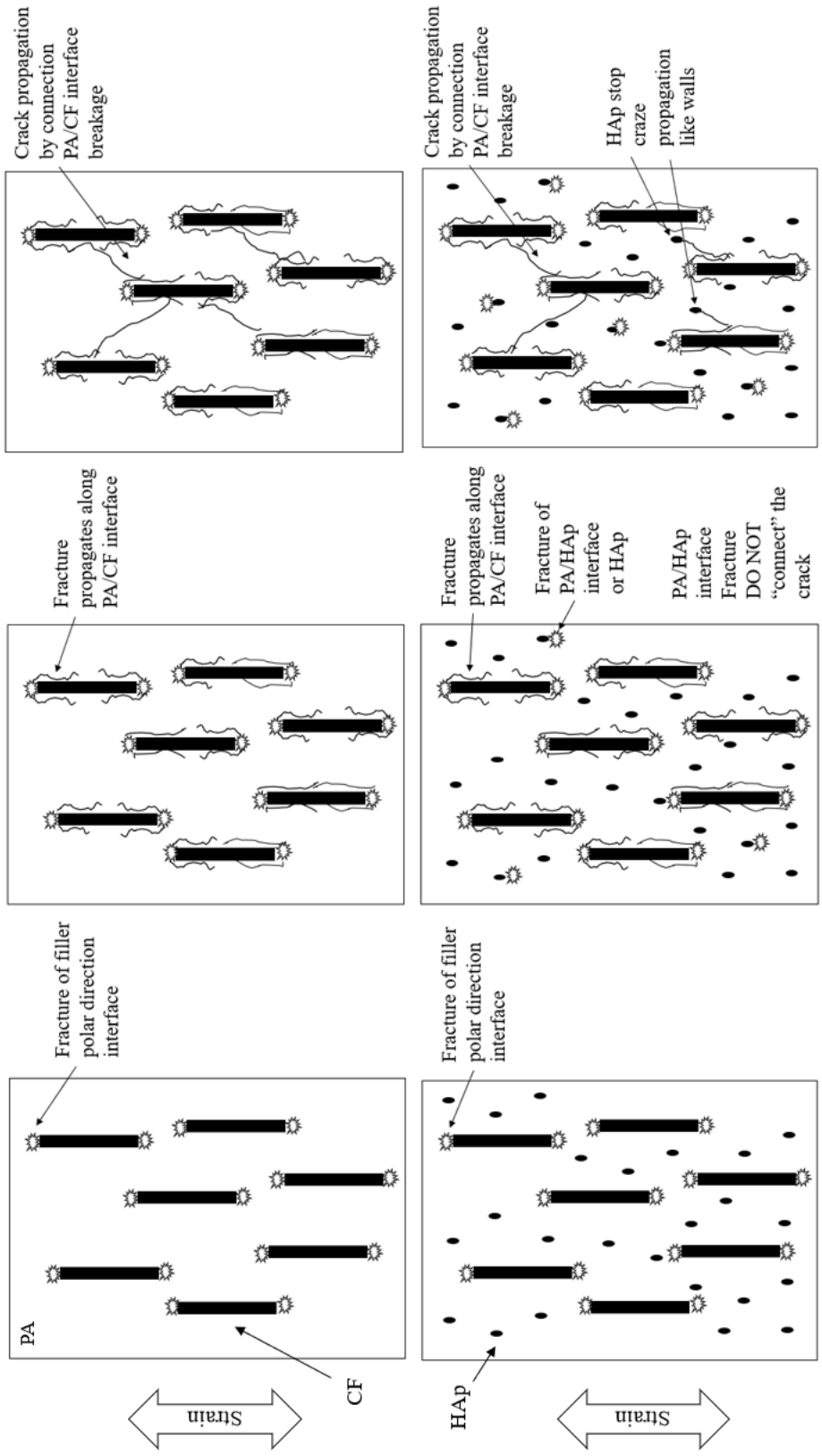

Fig. 3-9 Schematic illustration of PA/CF (upper row) or PA-HAp/CF (lower row) fracture behavior.

For PA/GF composite, fracture was also started at filler polar direction interface and matrix of near filler polar direction (initial craze formation stage). Then, the crack was formed (stable crack formation stage). Because the modulus difference of PA and GF was relatively small and interface adhesiveness was relatively large, the crack propagation occurred not only PA/GF interface but also matrix. At last, unstable crack propagation occurred before the fracture. For PA-HAp/GF composite, fracture was also started at filler polar direction interface and matrix of near filler polar direction (initial craze formation stage). In addition, the fracture of PA/HAp interface was occurred and the fracture part connected to the crack as the crack propagation proceed. The switching stress from stable crack formation to unstable crack propagation was decreased because of this crack connection effect of HAp. At last, unstable crack propagation occurred before the fracture.

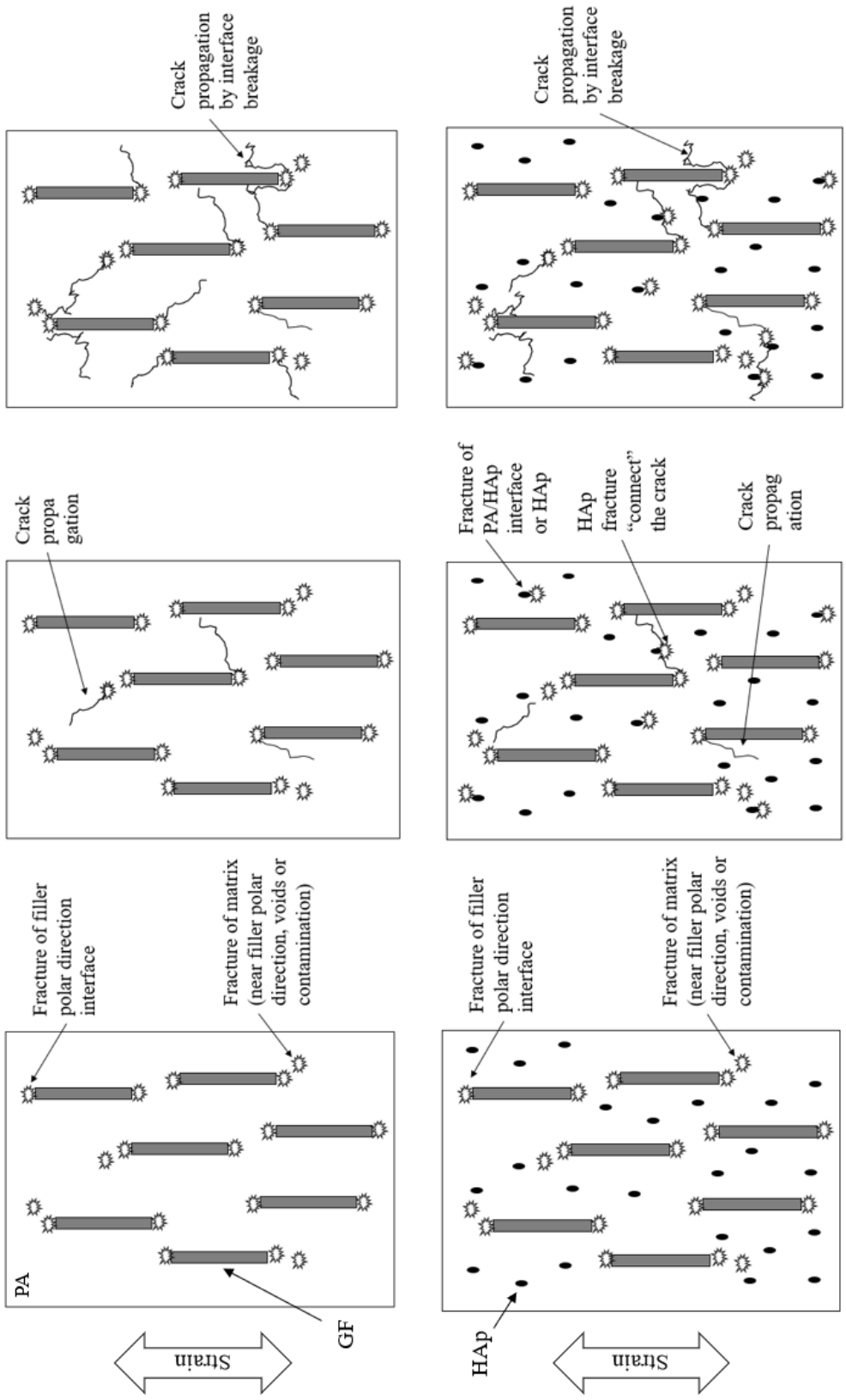

Fig. 3-10 Schematic illustration of PA/GF (upper row) or PA-HAp/GF (lower row) fracture behavior.

Conclusions

Fracture behavior of CF or GF reinforced PA-HAp nanocomposite was analyzed by AE and the effect of HAp was found to be different, which attributed to the difference of filler modulus and interface adhesiveness.

Critical stress of PA-HAp/CF AE event rapid increase and micro crack combination behavior was almost same as PA/CF composite. However, PA-HAp/CF AE energy rapid increase critical stress was larger than PA/CF composite, which attributed to the interfacial polymer of PA-HAp that undertook the part of the stress at the interface of PA/CF.

PA-HAp/GF composite behavior under stress was different from PA/GF composite. Critical stress of PA-HAp/GF AE event rapid increase was decreased by HAp. Once crack propagation started, interface of PA and HAp accelerated the fracture by acting as relay point of crack. This was because HAp was dispersed as nanosized particle and distance between each HAp was small.

The reason of this different effect of HAp was the difference of filler modulus and interface adhesiveness. This HAp effect also contributed the improvement of PA-HAp/CF creep resistance. Retention time until fracture was measured at tensile creep test and the time would be prolonged by increasing the critical stress of AE energy rapid increase. Interfacial polymer of PA-HAp or HAp itself shared the stress with PA/CF interface and prolonged the retention time until fracture. Creep property was a good index of material long term reliability. This was the first report that nano additive can increase the PA/CF composite creep property as far as we know.

References

[1] Rahimi, S. K.; Otaigbe, J. U. *Polymer Engineering and Science,* **2016**, *56* (9), 1045-1060.

[2] Rybnicek, J; Lach, R.; Schöne, J.; Tondl, D.; Dominguez, S. R.; Valek, R.; Grellmann, W. *Key Engineering Materials,* **2014**, *592*, 586-589.

[3] Mantia, F. P. L.; Mistretta, M. C.; Rodono, L.; Ascione, L.; Morreale, M. *Journal of Applied Polymer Science,* **2016**, *133* (44), 44180-44180.

[4] Noda, K.; Takahara, A.; Kajiyama, T. *Polymer*, **2001**, *42*, 5803-5811.

[5] Noda, K.; Tsuji, M.; Takahara, A.; Kajiyama, T. *Polymer*, **2002**, *43*, 4055-4062.

[6] Lee, L. H.;Mandell, J. F.; Mcgarry, F. J. *Polym. Eng. And Sci.,* **1987**, *27* (15), 1128-1136.

[7] Wyzgoski, M. G.; Novak, G. E. *Polym. Eng. And Sci.,* **1992**, *32* (16)*,* 1114-1125.

[8] Burford, R. P.; Benson, C. M. *Materials Forum*, **1995**, *19,* 129-144.

[9] Beheshtizadeh, N.; Mostafapour, A.; Abbasi, H. *Measurement Computers and Control,* **2019**, *136*, 608-614.

[10] Pacheco-Salazar*,* O. F.; Wakayama, S.; Sakai, T; Cauich-Rodriguez, J. V.; Rios-Soberanis, C. R.; Cervantes-Uc, *J. of the Mechanical Behavior of Biomedical Materials*, **2015**, *46*, 137-147.

[11] Pacheco-Salazar*,* O. F.; Wakayama, S.; Sakai, T; Rios-Soberanis, C. R.; Cauich-Rodriguez, J. V.; Cervantes-Uc, J. M. *J. of Mat. Sci.*, **2016**, *52* (12), 5635-5645.

[12] Jinen, E, *Eng. Fract. Mech.*, **1990**, *37* (6), 1183-1194.

[13] Jinen, E.; Ni, Q.; Ikeuchi, T. *Journal of the Japan Society of Mechanical Engineers A,* **1994**, *60* (579)*,* 2553-2560.

[14] Jinen, E.; Ni, Q.; Ikeuchi, T. *Journal of the Japan Society of Mechanical Engineers A,* **1994**, *60* (580)*,* 2702-2709.

[15] Jinen, E. *Eng. Fract. Mech.*, **1985**, *21* (1), 157-171.

[16] Karger-Kocsis, J; Czigany, T. *J. Mater. Sci.,* **1993**, *28* (9), 2438-2448.

[17] NISSAN ARC, “CFRP interlayer peeling process analysis by AE”, [online: http://www.nissan-arc.co.jp/service/006_F064.html]

Chapter 4,
Nanocomposite of polyamide and 1D (needle shape) hydroxyapatite

Introduction

To increase the mechanical property of PA-HAp nanocomposite, HAp shape control was influential means. For example, the larger the filler L/D is, the better the mechanical property (especially tensile strength) is. In this chapter, controlling the HAp shape to high L/D shape (needle shape) was focused to increase the mechanical properties of PA-HAp nanocomposite produced by one-pot synthesis. The goal of this study in this chapter is; first, to synthesize high L/D HAp (needle shape HAp) in pure water as model reaction of one-pot synthesis. Second, to synthesize PA66-needle shape HAp nanocomposite by one-pot synthesis.

Ions in HAp crystal are easily replaced by another ion and there are many HAp analogues in nature ("Apatite" comes from "confuse" in Greek because of those many analogues) [1]. For dental hygiene field, it is very important to understand the HAp ion replacing effect especially for caries prevention because HAp properties such as solubility or crystallinity was drastically changed by ion replacing. In previous studies for dental hygiene field, HAp shape change was already reported but those studies were mainly subjected to clarify HAp status in human body and HAp synthesis was conducted at 30-80 ºC, which was far too low temperature compared to one-pot synthesis [2-4]. Little has been reported on HAp synthesis with controlling its shape at high temperature such as over 200 ºC, which is PA66 synthesis condition. However, those previous studies indicated that additional ion could change HAp shape by ion substitution and it may be possible to synthesis needle shape HAp during one-pot synthesis based on those previous studies.

F^- is widely used for caries prevention and F^- application for partial fluorination of tooth HAp is common treatment. HAp solubility was drastically decreased by the very small amount F^- substitution (under 0.4 mmol/g) [4]. F^- effect for crystallinity was also studied and it was found that F^- showed the specific effect for HAp crystallinity. At first, added F^- increased crystallinity, then as the F^- amount was increased, the crystallinity was decreased. And then as the F^- amount was increased further, the crystallinity was increased (Fig. 4-1). F^- substitute OH^- in HAp and decrease a axis lattice constant because F^- stayed slightly different position as existing OH^- and stabilize the crystal structure (Fig. 4-1) [5-12]. When F^- replaced OH^- stoichiometrically, the crystallinity was increased. However, partially replaced crystal structure was complicated and previous studies discussed that the complexity was the reason of F^- specific effect for HAp crystallinity.

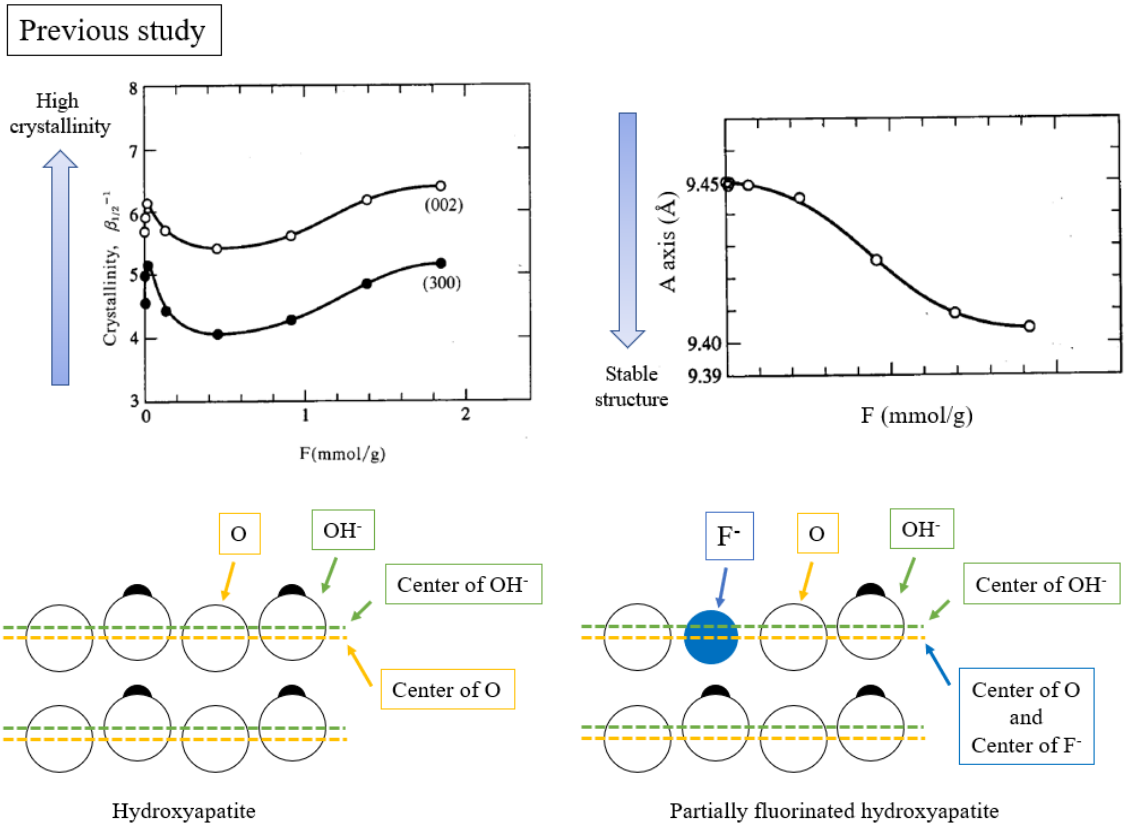

Fig. 4-1 Effect of F^- to HAp crystal structure. F^- could be settled in the more stable position than OH^- and stabilize the crystal structure especially the structure along a axis.

In the process of fluorinated HAp (fluorapatite; FAp) study, TEM images of partially fluorinated HAp was analyzed and some of them showed needle shape (Fig. 4-2) [4]. The reason was not explained but F^- specific effect for HAp crystallinity seemed to be the important factor. Needle shape HAp as FAp could be synthesized by using F^- effect.

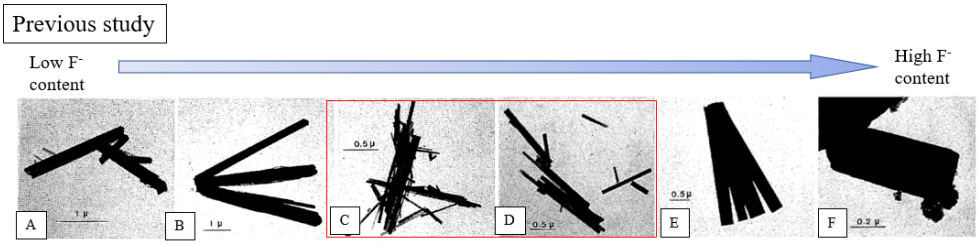

Product composition

	F (mM) feed	Ca (mmol/g)	P (mmol/g)	F (mmol/g)	(Ca/P) molar	TEM image
F_1	0	9.35	5.72	0	1.63	A
F_2	0.1	9.29	5.71	0.0121	1.63	B
F_3	0.2	9.38	5.72	0.0188	1.64	
F_4	1	9.25	5.71	0.134	1.62	C
F_5	5	9.53	5.72	0.441	1.67	D
F_6	10	9.32	5.65	0.920	1.65	
F_7	15	9.41	5.70	1.38	1.65	
F_8	20	9.27	5.59	1.85	1.66	E
F_9	50	9.16	5.37	2.28	1.71	
F_{10}	200	9.44	4.34	7.65	2.18	F

Fig. 4-2 Effect of F^- to HAp crystal growth. Needle shape HAp was generated by certain amount of F^- addition [4].

Previous studies also showed that when F^- was added, Ca/P ratio was the important factor for the HAp shape and HAp L/D increased as Ca/P decreased (Fig. 4-3) [4]. According to the literature, F^- replacing was adjusted by excess PO_4^{2-} at low Ca/P ratio. Appropriate F^- replacing amount and speed for needle shape HAp synthesis was facilitated by excess PO_4^{2-}. Ca/P ratio was the important factor to synthesize needle shape HAp (FAp) by using F^-.

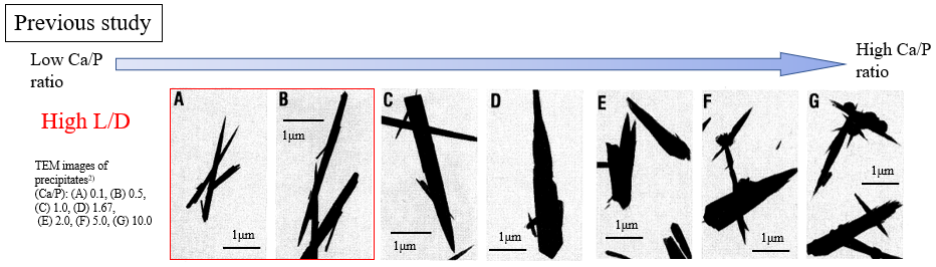

Feed solutions	Precipitates			
$(Ca/P)_f$, (mM/mM)	Ca (mmol/g)	P (mmol/g)	F (mmol/g)	TEM image
0.1=20/200	8.91	5.49	0.958	A
0.5=50/100	8.97	5.44	1.15	B
1=100/100	9.27	5.47	1.30	C
1.67=100/60	9.21	5.48	1.80	D
2=100/50	9.19	4.99	1.89	E
5=100/20	9.29	4.47	2.87	F
10=100/10	9.23	3.79	4.66	G

$(Ca/F)_f$=5.

Fig. 4-3 Effect of Ca/P ratio to HAp crystal growth. HAp L/D was increased as Ca/P ratio was decreased with coexisting F^- [4].

There are many hydroxyapatite analogues which contain Mg^{2+} in human body like enamel and dentin. Enamel contains less percentage of Mg^{2+} than dentin and showed higher crystallinity than dentin [13]. This indicated that Mg^{2+} could disarrange the HAp crystal array and decrease crystallinity. Previous study showed Mg^{2+} addition decelerate HAp synthesis. Mg^{2+} replaced Ca^{2+} and destabilized crystal structure (Fig. 4-4) [4, 14]. HAp containing Mg^{2+} showed irregular and partially amorphous shape.

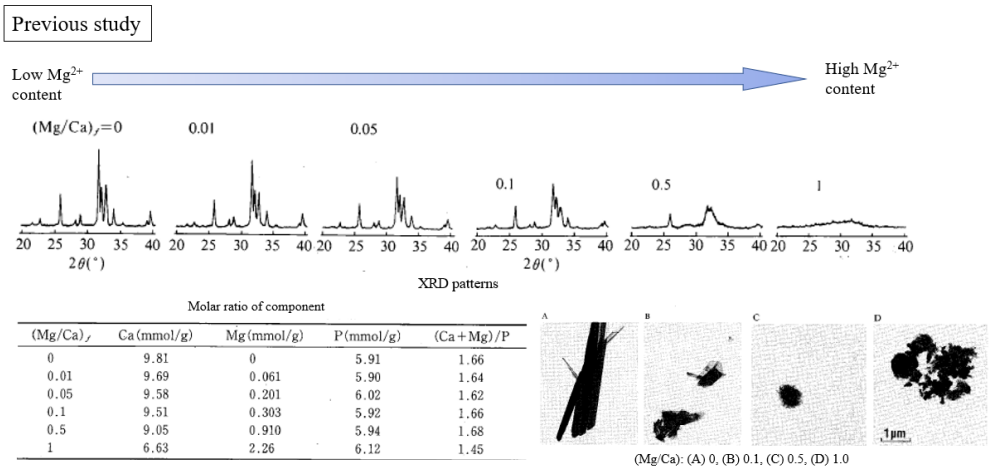

Fig. 4-4 Effect of Mg^{2+} to HAp crystal growth. HAp crystal growth was suppressed by Mg^{2+} addition [4].

However, when Mg^{2+} was used together with F^-, Mg^{2+} showed synergy effect with F^- and facilitate the needle shape HAp (FAp) synthesis (Fig. 4-5) [4]. Mg^{2+} replacement amount was increased as F^- amount was increased. Those ions were interacted with each other and changed the replacement ratio [15, 16]. Appropriate F^- replacing amount and speed for needle shape HAp synthesis was facilitated by Mg^{2+}. Mg^{2+} amount was also the important factor to synthesize needle shape HAp (FAp) by using F^-.

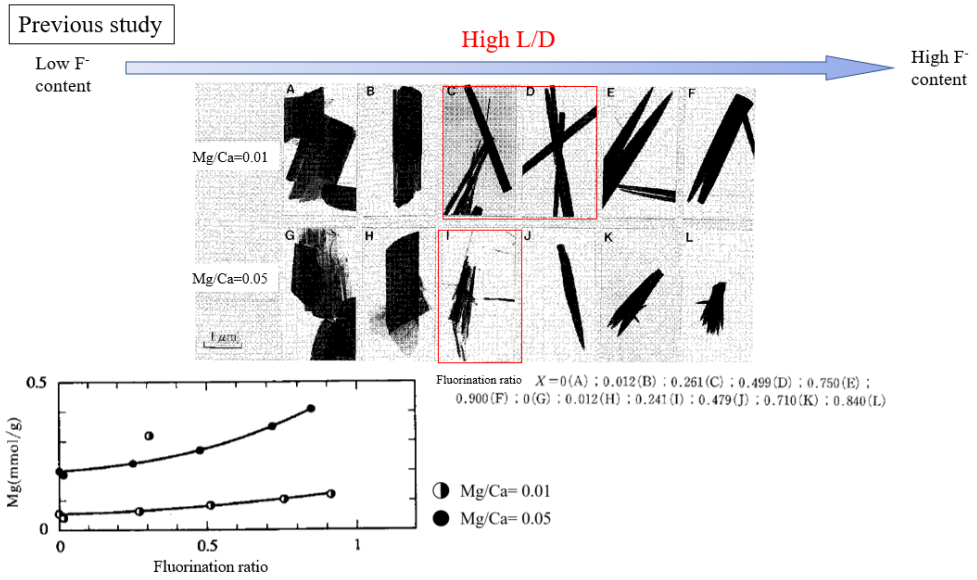

Needle shape HAp was generated by F^- ion and Mg^{2+} ion synergy effect.

Fig. 4-5 Effect of F^- and Mg^{2+} to HAp crystal growth. High L/D needle shape HAp was generated by F^- and Mg^{2+} synergy effect [4].

Those previous studies were mainly conducted at 80 ºC and showed that needle shape HAp could be generated at optimum ion composition under moderate temperature (80 ºC). F^- amount was the most important factor to generate the needle shape HAp. Ca/P ratio and Mg^{2+} amount was also important to change the F^- substitution ratio or speed to HAp and increase the L/D (Fig. 4-6).

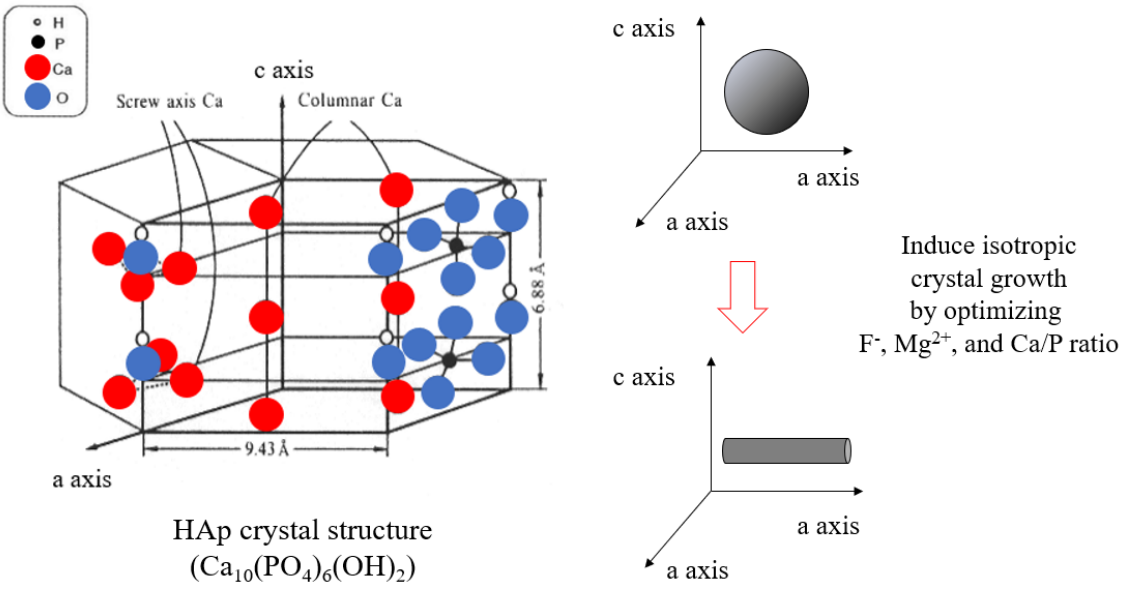

Fig. 4-6 Schematic illustration of the strategy to synthesize needle shape HAp.

At first, we tried to synthesize the needle shape HAp at high temperature (250 ºC) based on those previous studies in pure water as model reaction. Then, one-pot synthesis was carried out to produce PA-needle shape HAp nanocomposite under optimized condition.

Conclusions

Needle shape HAp (FAp) was synthesized during one-pot synthesis by adding F^- and Mg^{2+} ion compound to raw materials as well as optimizing the Ca/P ratio, which facilitated the isotropic HAp crystal growth. F^- accelerated the isotropic crystal growth which led the needle shape HAp growth. Mg^{2+} and optimized Ca/P ratio facilitated the effect. PA66-needle shape HAp (FAp) nanocomposite was obtained and the composite showed the increased mechanical properties as expected. Because of the high L/D filler, tensile strength was especially increased compare to PA-spherical shape HAp nanocomposite. It is the big advantage of one-pot synthesis that filler shape could be controlled during the synthesis by the optimization of raw materials.

References

[1] Wazer, J. R. V. *Phosphorus and Its Compounds*, Interscience, New York, **1958**.

[2] Bonfeild, W; Behri, J. C.; Doyle, C.; Bowman, J.; Abram, J. *Biomater. Biomech,* **1983***,* 421-426.

[3] Antonis, G. M.; Lyman, M. D.; Freed, L. E.; Langer, R. *Biomaterials,* **1994***, 15*, 55-58.

[4] Okazaki, M. (Eds.), *Chemistry of Apatite,* Tokai Univ.: Tokyo, **1993**.

[5] Naray-Szabo, S. *Z. Kristallogr,* **1930**, *75,* 387-398.

[6] Young, R. A.; Lugt, W.; Elliott, J. C. *Nature,* **1969**, *223*, 729-730.

[7] Okazaki, M.; Aoba, T.; Doi, Y.; Takahashi, J.; Moriwaki, Y. *J. Dent. Res.,* **1981**, *60,* 845-849.

[8] Okazaki, M.; Takahashi, J.; Kimura, H. *Caries Res.,* **1984**, *18*, 499-504.

[9] Moreno, E. C.; Kresak, M.; Zahradnik, R. T. *Nature,* **1974**, *247*, 64-65.

[10] Moreno, E. C.; Kresak, M; Zahradnik, R. T. *Caries Res.* **1977**, *11* (Suppl. 1), 142-171.

[11] Napper, D. H.; Smythe, B. M. *J. Dent. Res.,* **1966**, *45,* 1775-1783.

[12] Amjad, Z.; Nanollas, G. H. *Caries Res.,* **1979**, *12,* 250-258.

[13] Okazaki, M.; Takahashi, J.; Kimura, H. *J. Osaka Univ. Dent. Sch.,* **1984**, *24*, 13-20.

[14] Okazaki, M.; Takahashi, J.; Kimura, H. *Caries Res.,* **1986**, *20*, 324-331.

[15] McCann, H. G.; Bullock, F. A. *J. Dent. Res.,* **1957**, *36,* 391-398.

[16] Marier, J. R.; *Proc. Finn. Dent. Soc.,* **1980**, *76*, 93-102.

Chapter 5,
Nanocomposite of polyamide and 2D (plate shape) hydroxyapatite

Introduction

One-pot hydrothermal synthesis of PA and HAp was carried out to produce PA-HAp nanocomposite (chapter 2). HAp shape in the PA66-HAp nanocomposite reported in chapter 2 was spherical shape. In general, spherical shape which has a low L/D filler shows relatively small effect to increase mechanical properties for injection molded plastics. A plate shape filler is expected to increase the mechanical properties like flexural strength and flexural modulus. To increase those properties by filler shape modification, synthesis procedure of plate shape HAp was investigated.

Wang et al. studied calcium orthophosphates and showed that octa-calcium phosphate (OCP) was HAp precursor, which had the plate-like shape [1]. Aoba et al. reported the plate shape OCP synthesis and plate shape HAp synthesis from OCP [2]. Monma suggested that OCP changed to HAp by heterogeneous reaction via Ca-deficient hydroxyapatite (CDHA) by heating [3]. Brown et al. studied OCP crystal structure and transition mechanism from OCP to HAp in detail [4]. Fig. 5-1 showed the proposed process of HAp formation from OCP. OCP had the layer structure which was constructed by calcium phosphate type layer and water rich layer. The calcium ion arrangement in calcium phosphate type layer of OCP resembled HAp structure and the layer was expected to become HAp by dehydration reaction. HAp was formed by OCP hydrolysis and HAp shape partially reflected OCP shape.

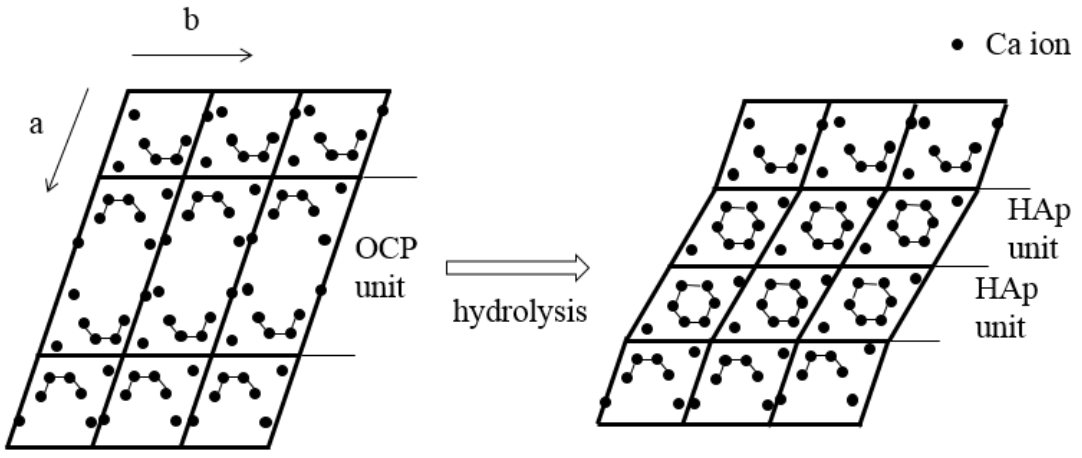

Fig. 5-1 Proposed process of HAp formation from OCP which shows the dehydration of OCP water layer and HAp synthesis by remaining HAp layer (heterogeneous reaction) [4].

According to those previous studies, OCP was chosen as intermediate to synthesis plate shape HAp in this study. However, previous studies also showed it is difficult to synthesis OCP with high purity and yield because the continuous control of pH and ion density was needed to synthesis OCP. In addition, OCP was not stable and easily converted to HAp even during the OCP synthesis [4-7]. Liu et al. studied the effect of temperature and pH for OCP synthesis and reported that pH range suitable for OCP synthesis was narrow [6]. If the pH was too low, OCP could not be obtained as precipitate. On the contrary, OCP was easily converted to HAp at high pH and only the mixture of OCP and HAp was obtained. Ban et al. studied the effect of temperature and reaction time for OCP synthesis [7]. They reported that OCP generation from $CaHPO_4 \cdot 2H_2O$ (DCPD) and HAp synthesis from OCP occurred as sequential reaction. When the temperature was under 40 ºC, the reaction yield of OCP generation from DCPD was low. They also reported that the crystallinity of OCP which obtained at under 40 ºC was low. On the contrary, when the temperature was over 70 ºC, generated OCP was quickly converted to HAp. They concluded that the temperature range from 50 ºC to 60 ºC was appropriate reaction temperature to obtain OCP.

Ban et al. also reported as the patent that calcium and phosphorus ratio (Ca/P) was important factor to obtain OCP at high yield [8]. When the raw material Ca/P ratio was OCP stoichiometric ratio (Ca/P =1.33), they reported the maximum 98 wt% OCP yield.

Graham et al. conducted HAp synthesis from OCP through increasing pH and Ca^{2+} density by adding calcium hydroxide or tetracalcium phosphate [5]. Aoba et al. reported the plate shape HAp synthesis from OCP under the condition of 160 atm to 180 atm at 200 ºC for 2 days to 7 days [2]. Little has been reported on OCP conversion to HAp with organic molecular like amine or acid, which is PA66 monomer.

In this chapter, OCP was focused as HAp raw material to synthesize PA-plate shape HAp nanocomposite by one-pot synthesis and the synthesis condition was studied. At first, OCP synthesis and HAp synthesis from OCP was investigated to use OCP as HAp raw material. Then one-pot synthesis with OCP was carried out and the reaction process was studied.

Conclusions

PA-plate shape HAp nanocomposite was synthesized from PA66 monomers and OCP by one-pot synthesis. Resultant HAp was plate shape by reflecting the precursor OCP shape because OCP conversion reaction to HAp was heterogeneous. PA affinity for HAp in PA-plate shape HAp nanocomposite was improved by intercalating ADA to OCP during one-pot synthesis. The ADA acted as bound polymer precursor. It was found that plate shape HAp increased material strength especially flexural strength and reduced water absorption rate.

References

[1] Wang, L.; Nancollas, G. H. *Chem. Rev.*, **2008**, *108*, 4628-4669.

[2] Aoba, T; Ishida, T.; Tagi, T.; Hasegawa, K; Moriwaki, Y. *Jap. J. oral Biol.*, **1975**, *17*, 1-7.

[3] Monma, H. *J. Mater. Sci.* **1980**, *15* (19), 2428-2434.

[4] Brown, W. E.; Mathew, M.; Tung, M. S. *Prog. Crystal Growth Charact*., **1981**, *4,* 59-87.

[5] Graham, S; Brown, P. W. *J. Crystal Growth,* **1996**, *165* (1), 106-115.

Chapter 6,
General conclusions

In this study, we investigated the synthesis, morphology, and property of PA-HAp nanocomposite. PA properties, especially mechanical properties were improved by nanofiller reinforcement. This study is distinguished from the previous studies in terms of;

1, Autonomous synthesis of nanocomposite from micro size raw material.

2, Autonomous strong interface creation between matrix and filler.

3, Controllable filler shape such as 0D (sphe), 1D (needle), and 2D (plate).

Nanocomposite of PA66 and HAp which showed those features was produced by novel synthesis process.

In chapter 2, PA-0D (spherical shape) HAp nanocomposite was synthesized. The conventional melt kneading method could not produce PA-HAp nanocomposite with desired features due to filler aggregation. To solve the problem and enable the autonomous synthesis of nanocomposite from micro size raw material, and autonomous strong interface creation between matrix and filler, the simultaneous synthesis of HAp and PA66 in one reaction vessel was carried out. We called this new scheme as “one-pot synthesis.” This is the first study which tries to synthesize HAp with PA66 under the high temperature polymerization condition. In addition, previous studies indicated that an organic molecular like PA66 monomer may inhibit the HAp synthesis. To clarify the HAp synthesis under polymerization condition, HAp synthesis under various conditions was investigated at first. Fortunately, in the range of PA66 polymerization condition, HAp stable synthesis was confirmed.

Then, simultaneous synthesis of HAp and PA66 (one-pot synthesis) was carried out. A precedent HAp synthesis followed by PA66 polymerization was occurred. The HAp raw material was micro meter size, much larger than resultant nanosized HAp. Nanocomposite was produced autonomously from micro meter raw material by one-pot synthesis and the reaction mechanism was clarified. In addition, the autonomous bound polymer formation between HAp and PA66 during one-pot synthesis was confirmed. The amount of bound polymer was greater than that achieved by conventional melt kneading and that rich bound polymer enabled the HAp fine dispersion in the PA-HAp composite. Properties of nanocomposite produced by one-pot synthesis were evaluated and it was found that the PA-HAp nanocomposite showed many improved properties than neat PA. Although one-pot synthesis was easy, economical method compare to other nanocomposite synthesis method, this method could produce a fine nanocomposite comparable to other nanocomposites.

In chapter 3, we found that CF reinforced PA-HAp nanocomposite showed the improved tensile strength, tensile toughness, and tensile creep resistance than CF reinforced PA. The reason was the difference of modulus and interface adhesiveness between CF and HAp. Because of the excellent HAp dispersion and strong interface adhesiveness enabled by one-pot synthesis, HAp could improve the

mechanical properties and creep resistance of the composite. Long-term reliability evaluated by creep resistance was one of the most desirable features for industrial usage, and as far as we know this was the first report that nanofiller could improve the PA/CF composite creep resistance.

In chapter 4, PA-1D (needle shape) HAp nanocomposite was synthesized. Previous studies suggested that the additional ion to HAp raw material may change the resultant HAp shape by partial ion substitution and isotropic HAp crystal growth. At first, to obtain the needle shape HAp, additional ion effect for the HAp shape formation was studied. HAp shape was changed by adding F^- to HAp raw material, which accelerate the anisotropic HAp crystal growth by partial ion substitution. Adding Mg^{2+} and optimize Ca/P ratio facilitated the effect. Then under optimum ion composition, PA-needle shape HAp nanocomposite was obtained by one-pot synthesis. The composite showed increased mechanical properties, especially high tensile strength because of the high L/D filler.

In chapter 5, PA-2D (plate shape) HAp nanocomposite was synthesized. Octa-calcium phosphate (OCP) was focused as reaction intermediate to HAp, which had the plate shape and was expected to convert HAp heterogeneously. At first, one-pot synthesis with OCP was conducted and PA-plate shape HAp nanocomposite was synthesized. However, the interface between matrix and plate shape HAp was poor due to the low interaction of OCP and PA66 monomer. Then, adipic acid (ADA) intercalated OCP was used as HAp precursor to accelerate the bound polymer formation. Resultant PA-plate shape HAp nanocomposite showed the better PA affinity for HAp because intercalated ADA partially became the foundation of bound polymer. The PA-plate shape HAp nanocomposite showed increased mechanical properties, especially flexural properties, and reduced water absorption rate.

In summary, the novel nanocomposite was synthesized by simple and economical method which was suitable for industrial mass production. This material is expected to expand PA market.

Publications

[1] Okumura, T.; Sonobe, K.; Ohashi, A.; Watanabe, H.; Watanabe, K.; Oyamada, H.; Aramaki, M.; Ougizawa, T. Synthesis of Polyamide-Hydroxyapatite Nanocomposites. (Accepted on 24 April, 2020 by Polymer Engineering & Science).

[2] Okumura, T.; Sonobe, K.; Ohashi, A.; Watanabe, H.; Watanabe, K.; Oyamada, H.; Noda, K.; Aramaki, M.; Ougizawa, T. Mechanical Properties and Fracture Behavior of Fiber Filler Reinforced Polyamide-Hydroxyapatite Nanocomposite. (Submitted).

[3] Okumura, T.; Sonobe, K.; Ohashi, A.; Watanabe, H.; Watanabe, K.; Oyamada, H.; Aramaki, M.; Ougizawa, T. Properties of Polyamide-Hydroxyapatite Nanocomposites. (To be submitted).